Journal of Hydrology 381 (2010) 308–321

Contents lists available at ScienceDirect

Journal of Hydrology

journal homepage: www.elsevier.com/locate/jhydrol

An integrated framework for the hydrologic simulation of a complex geomorphological river basin

Nektarios N. Kourgialas, George P. Karatzas *, Nikolaos P. Nikolaidis

Technical University of Crete, Department of Environmental Engineering, Polytechneioupolis, 73100 Chania, Greece

ARTICLE INFO

Article history:
Received 11 February 2009
Received in revised form 29 October 2009
Accepted 3 December 2009

This manuscript was handled by P. Baveye, Editor-in-Chief, with the assistance of Chris Soulsby, Associate Editor

Keywords:
Surface flow modeling
HSPF model
Karstic modeling
Energy Budget Snow Melt
GIS
Koiliaris River Basin

SUMMARY

The purpose of this study was to simulate the surface and groundwater flow in a karstic river basin where flood phenomena appear from time to time. The Koiliaris River Basin is located east of the city of Chania on the island of Crete in Greece. This river basin has a complex hydrogeology that consists of temporary – ephemeral rivers (tributaries), high mountainous karstic areas, springs, downstream karstic areas and karstic channel parts. In order to simulate all of these processes, a combination of four models was employed. The four models used in the present study were: (a) a two-part Maillet karstic model, used to determine the spring discharge, (b) a GIS-based Energy Budget Snow Melt model, developed to simulate the snow melt rate and compute the snow melt flow that enters the karstic system of the high mountainous area, A matlab code developed in this work combines the previous two independent models, (c) an empirical karstic channel model, developed to simulate the flow in the downstream karstic part of the Koiliaris River Basin, and (d) the Hydrological Simulation Program – FORTRAN (HSPF) model was used to model the hydrology of the watershed. Besides the karstic model, developed in this work, a significant contribution is that for the computation of the snow melt rate the energy budget considers the topography of the area (using GIS) that is incorporated with seven important parameters: elevation, slope, curvature, aspect, illumination, land use, and radiation. The main steps of this study included calibration, validation and sensitivity analysis of the HSPF model. The simulated results are in a very good agreement with the observed field data.

Introduction

One of the main disadvantages of the models estimating the river flow is the fact that in many cases the contribution of the groundwater flow is ignored. The contribution of the subsurface flow can be significant in areas with a karstic geological formation. In karstic areas most of the surface runoff and the snowmelt water become groundwater flow which can appear in the downstream direction in the form of springs. In other cases, this groundwater flow becomes a significant contribution to the main river flow (Jaquet et al., 2004). Modeling of groundwater flow in karstic aquifers remains a complex task that has not been very successful in the past (White, 2002). Karstic river basins have several peculiarities and are difficult to model as the contribution of the subsurface flow can be a significant portion of the total flow that has a complex behaviour. A large number of temporary – ephemeral rivers are located in karstic areas where their base flow comes from spring discharges. The karstic base flow, which can not be modeled by traditional watershed models, comprises an important component of river hydrology and should be included in the hydrologic models. In some cases, parts of a temporary river – ephemeral consist of a karstic channel geomorphology that needs to be considered in a hydrologic simulation. Recently, Viswanathan et al. (2005) and Tzoraki and Nikolaidis (2007) attempted to use HSPF modeling to describe the hydrology of karstic watersheds.

Apart from the karstic flow, the snow melt rate also plays a significant role to the river flow (Albek et al., 2004). In most of the previous studies the estimation of the snow melt was based on a melt index approach (empirical equations), with the most common to be the degree-day method, where air temperature is used to index all of the energy fluxes (Bras, 1989). In some other studies the amount of snow melt was computed using an energy budget model, where the energy balance equation was used to simulate the energy fluxes within the snow pack (Mazurkiewicz et al., 2008; Sensoy et al., 2006; Ganju et al., 1999). In all the previous studies the influence of the topography on the snow melt rate was ignored. Snowmelt is very important in surface water hydrology, groundwater hydrology and flood control. As Anderson (1968) stated the only way to correctly compute the snow melt rate is the energy budget. The main contribution of the present work is that the computation of snow melt rate is computed using the energy budget

* Corresponding author.
E-mail address: karatzas@mred.tuc.gr (G.P. Karatzas).

0022-1694/$ - see front matter © 2009 Elsevier B.V. All rights reserved.
doi:10.1016/j.jhydrol.2009.12.003

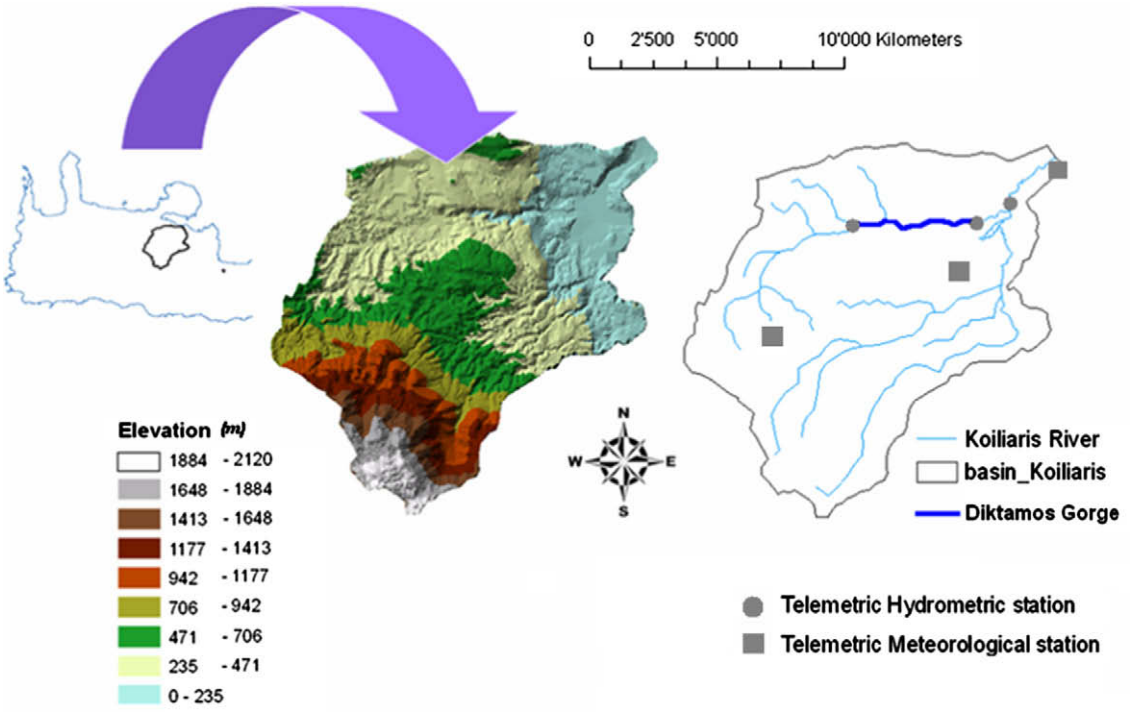

Fig. 1. The geomorphology of the Koiliaris River Basin and the hydrometeorological network.

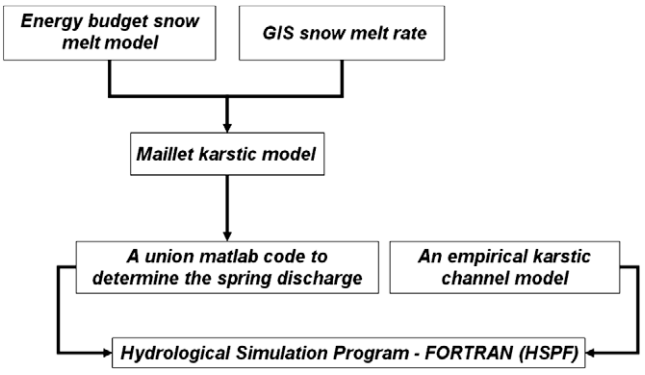

Fig. 2. A graphical representation of the models that were connected in a union hydrologic framework.

that takes into consideration the topography of the area using GIS. Specifically, for the karstic area above 900 m (where snow melt takes place) the topography of the area is considered using seven important parameters: (1) the elevation, (2) the slope, (3) the curvature, (4) the aspect, (5) the illumination, (6) the land use, and (7) the radiation. The main objective of this study was to develop a modeling framework to simulate the hydrologic regime of a complex geomorphological environment where snow melt takes place and is located at the Koiliaris River Basin (Fig. 1). For this purpose, the HSPF model was combined with a karstic GIS Energy Budget Snow Melt model and an empirical karstic channel model which were developed in this study in order to compute the surface and groundwater flow contributions to the Koiliaris River flow (Fig. 2). The obtained simulation results were compared to field measurements.

Koiliaris River Basin

The Koiliaris River Basin is located 15 km east of the city of Chania in Crete. The basin extends from the White Mountains (Lefka Ori) to the coastline. The area of the basin has been estimated to be approximately 130 km^2. The elevations of the basin range from 0 to 2120 m MSL. The total length of the hydrologic network of the Koiliaris River is 36 km. There are three telemetric hydrometric stations and three telemetric meteorological stations in the river basin as shown in Fig. 1.

The topography of the area of interest is smooth with a mild topographic slope of 12%. The geology of the basin is mainly constituted by carbonate, quaternary-neogenic deposits and flysch formations. Based on a study conducted by the Ministry of Agriculture of Greece, it has been estimated that 58% of the total land use of the basin is characterized as pasture (public or private), 29.4% as crops, 2.8% as settlements and roads, 8.5% as forests, 0.6% as water surfaces and 0.7% as land for other uses.

The meteorological data used in this study cover the time period 1975–2008. In the basin there are three telemetric hydrometric stations and three telemetric meteorological stations shown in Fig. 1. These stations were installed in the summer of 2007 and operated by the Technical University of Crete. The data from the stations were selected and recorded hourly. The data for the years up to 2007 were obtained from the four surrounding stations. These stations are evenly distributed regarding altitude and land-planning and have continuously collected measurements of meteorological parameters for a long period of time.

Methodology – The conceptual model

The karstic model

The main volume of water in the area of study is discharged from the karstic system of the White Mountains (Lefka Ori) through springs, streams and temporary – ephemeral rivers. The main karstic discharge point in the Koiliaris River Basin is the Stylos Spring (Fig. 4). The Stylos Spring is one of the main water sources of the area and the major discharge point of the karst system of White Mountains.

The karstic model used was based on a two reservoir Maillet model (Maillet, 1905). Maillet's model was selected because it uses the hydrologic balance equation during the recession period. The karstic system of the Koiliaris River was considered as a two reservoir system (Stamati et al., 2006). The analysis of the above system suggests the existence of two reservoirs within the karstic system; the upper reservoir with a faster response (wide conduits), and the lower reservoir with a slower response (narrow fractures). A two-part Maillet model was employed representing the upper and lower reservoirs (Fig. 3).

Two hydrologic balance equations were developed representing the upper and lower reservoirs. Fig. 3 presents the concept of the karstic model and its hydrologic pathways. The rate of change of the water volume in the upper reservoir V_{up} is equal to the daily inflow of water to the reservoir $Q_{in,up}$ minus the daily outflow from the reservoir Q_{up}:

$$\frac{dV_{up}}{dt} = Q_{in,up} - Q_{up}. \quad (1)$$

Similarly for the lower reservoir:

$$\frac{dV_{lower}}{dt} = Q_{in,lower} - Q_{lower}. \quad (2)$$

The daily inflows of water to the upper and lower reservoirs can be calculated from the following equations:

$$Q_{in,up} = a_1 Q_{in} = a_1 \times (P_w + M_s) \times \varepsilon \times A_{Karst}, \quad (3)$$

$$Q_{in,lower} = (1 - a_1)Q_{in} + a_2 Q_{up} = (1 - a_1) \times (P_w + M_s) \times \varepsilon \times A_{Karst} + a_2 Q_{up}, \quad (4)$$

where a_1 is the fraction of the precipitation and snow melt total flow entering the upper reservoir, Q_{in} is the initial discharge that enters the karstic system by rain and snow melt, a_2 is the fraction of

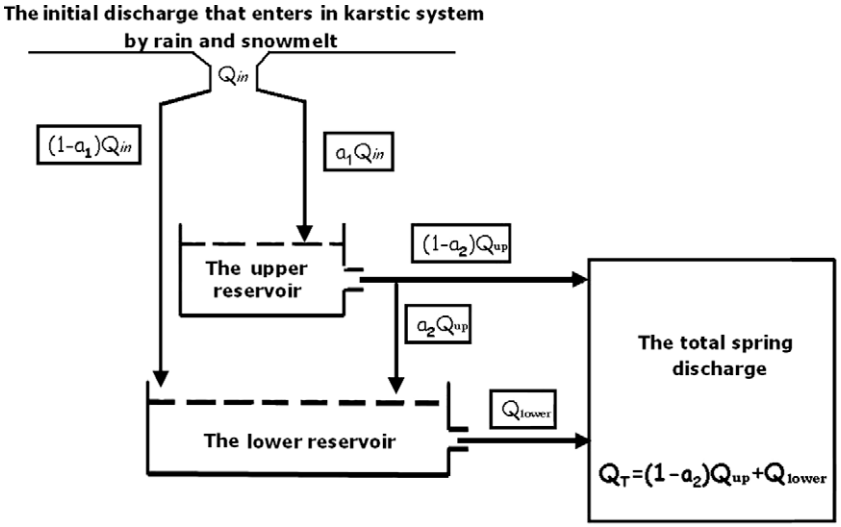

Fig. 3. The conceptual karstic model.

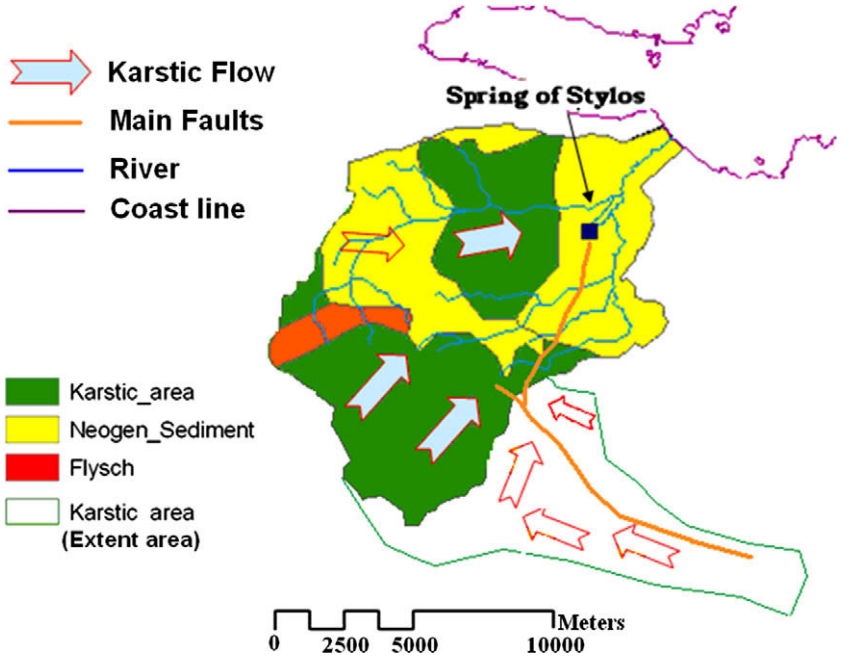

Fig. 4. The Stylos Spring and the extent karstic area of the Koiliaris River Basin.

the upper reservoir discharge entering the lower reservoir (Fig. 3), P_w is the daily precipitation (m/d), M_s is the daily snow melt rate (m/d) (its analytical calculation is presented in Section "The Energy Budget Snow Melt model"), ε is an adjustment factor that accounts for the hydrologic abstractions of the snow, and A_{Karst} is the karstic area (m^2). Assuming $Q_{in,up}$ constant the analytical solution of Eq. (1) yields:

$$\lambda_1 \frac{dQ_{up}}{dt} + Q_{up} = Q_{in,up} \Rightarrow \frac{dQ_{up}}{dt} + \frac{1}{\lambda_1} Q_{up} = \frac{Q_{in,up}}{\lambda_1}$$
$$\Rightarrow Q_{up} = Q_{up-1} e^{-\frac{t}{\lambda_1}} + e^{-\frac{t}{\lambda_1}} \int \frac{Q_{in,up}}{\lambda_1} e^{\frac{t}{\lambda_1}} dt$$
$$\Rightarrow Q_{up} = Q_{up-1} e^{-\frac{t}{\lambda_1}} + \frac{Q_{in,up}}{\lambda_1} e^{-\frac{t}{\lambda_1}} \int e^{\frac{t}{\lambda_1}} dt$$
$$\Rightarrow Q_{up} = Q_{up-1} e^{-k_u t} + Q_{in,up}(1 - e^{-k_u t}).$$

Similarly, the analytical solution of Eq. (2) yields:

$$Q_{lower} = Q_{lower-1} e^{-k_l t} + Q_{in,lower}(1 - e^{-k_l t})$$

Therefore, considering Eqs. (3) and (4) we obtain:

$$Q_{up} = Q_{up-1} e^{-k_u t} + a_1 Q_{in}(1 - e^{-k_u t}), \quad (5)$$
$$Q_{lower} = Q_{lower-1} e^{-k_l t} + [a_2 Q_{up} + (1 - a_1) Q_{in}](1 - e^{-k_l t}), \quad (6)$$
$$Q_T = (1 - \alpha_2) \times Q_{up} + Q_{lower}, \quad (7)$$

where Q_T is the total spring discharge, Q_{up} and Q_{lower} as previously defined, Q_{up-1} is the value of Q_{up} at the previous time step, $t - 1$, $Q_{lower-1}$ is the value of Q_{lower} at the previous time step, $t - 1$, and k_u, k_l, $(1/d)$ are the recession coefficients of the upper and lower reservoirs, respectively. The time step t of the model is equal to 1 day (Tzoraki and Nikolaidis, 2007). Parameter Q_{in} includes the rainfall and the daily snow melt rate. In the case of the Koiliaris River Basin, the runoff data for the dry period of 2005 and 2006 were used for the calibration and validation of the karstic flow model (Stamati et al., 2006).

The Stylos Spring discharges at 17 m MSL with the discharge presenting intense seasonal fluctuations. The karstic model takes as input precipitation and snow melt and is calibrated against field discharge time series by adjusting the model parameters.

Due to the lack of previous data, a geological study was performed in order to determine the karstic area. Based on this study, there exist two main karstic faults in the area of interest. These faults are connected as shown in Fig. 4 and lead directly to the Stylos Spring. The estimated extended karstic area that contributes to the discharge of the Stylos Spring is shown in Fig. 4 (Kourgialas et al., 2008). In order to determine the total spring discharge Q_T, it is necessary to estimate the daily snow melt rate M_s, which is computed by using the Energy Budget Snow Melt model as described in the next section.

The Energy Budget Snow Melt model

General information about the process of snow melt

The mountainous area of the Koiliaris River Basin has a karstic geomorphology, thus the main volume of snow melt inserted into the karstic system is discharged to the Stylos Spring. An Energy Budget Snow Melt model was used to calculate the snow melt rate M_s in Eqs. (3) and (4). In contrast to rainfall, snowfall has a delayed effect on river flow and hydrology. Snow melt waters are crucial for water supply and can also cause serious floods, particularly when compounded with spring rainfalls (Anderson, 1973). Air temperature is the main parameter that characterizes the form of precipitation from rain to snow. The critical temperature at which precipitation changes from rain to snow is 2.2 °C (Yang and Dickinson, 1997). In addition to air temperature, altitude is a critical factor for snow melt. Snowfall usually increases with altitude and it usually appears at altitudes greater than 900 m (Dingman, 1994).

Energy Budget Snow Melt model

The density of snow pack increases with depth and as the accumulation season progresses. As snowfall continues, the new depth of snow pack becomes

$$D_2 = D_1 - \Delta D + D_N, \quad (8)$$

where D_1 and D_2 are the old and new depths of snow pack (cm), respectively, D_N is the depth of new snow (cm) and ΔD is the change in depth due to the compaction by the snow (cm). The mathematical expression for the snow depth change is given (Bras, 1989) by:

$$\Delta D = 2.54 \times \frac{P \times D}{WE} \times \left(\frac{D}{10}\right)^{0.35}, \quad (9)$$

where P is the water equivalent of new snow, a function of its density, D is the present snow-pack depth (cm) and WE is the water equivalent of snow pack, a function of its density. The density of water is considered equal to 1 g/cm^3.

The depth of new snow D_N in Eq. (8) is expressed as

$$D_N = \frac{P}{P_N}, \quad (10)$$

where the density of new snow P_N (g/cm^3) is expressed as

$$P_N = 0.05 + (T_a/100)^2 \quad \text{if} \quad T_a > 0\ ^\circ\text{C}, \quad (11)$$
$$P_N = 0.05 \quad \text{if} \quad T_a \leqslant 0\ ^\circ\text{C} \quad (12)$$

and T_α is the air temperature (°C) in the area of interest (recorded from the meteorological station 3 m above the ground).

The water equivalent of snow pack is expressed as

$$WE_2 = WE_1 + P, \quad (13)$$

where WE_2 and WE_1 are the new and old values, respectively.

The new snow-pack density relative to water is

$$p_{p2} = \frac{WE_2}{D_2}. \quad (14)$$

The energy budget at any given time interval can be expressed (Ohara and Kawas, 2005) as:

$$Q_0 = R_N + Q_V - Q_e - Q_h - Q_g + Q_f, \quad (15)$$

where Q_0 = change in heat storage [J/(cm^2 day)], R_N = net radiation exchange [J/(cm^2 day)], Q_V = advected heat by precipitation [J/(cm^2 day)], Q_e = heat consumed in evaporation and sublimation [J/(cm^2 day)], Q_h = sensible-heat transfer by turbulent convection [J/(cm^2 day)], Q_g = ground-snow exchange by conduction [J/(cm^2 day)], and Q_f = energy released by the freezing of any liquid water in the snow pack [J/(cm^2 day)]. The thermal quality Θ is defined as the ratio of Q_0 to the energy Q consumed in producing the same amount of melt from pure ice at 0 °C. This latter quantity is:

$$Q = p_p D L_m \quad (16)$$

where: L_m = 334.72 J/g is the latent heat of ice melting, p_p = snow-pack density as a function of the depth (g/cm^3). Based on the above, the thermal quality Θ expressed as the ratio of Eqs. (15) and (16), (Bras, 1989) is:

$$\Theta = \frac{Q_0}{Q}, \quad (17)$$

Typical values of the thermal quality range from 0.95 to 1.0. The thermal quality of the snow is affected by temperature according to the follow relationships:

$\Theta = 1$ for $T_\alpha < 0\,^\circ C$, $\Theta = 0.99$ for $0\,^\circ C \leqslant T_\alpha \leqslant 1\,^\circ C$,
$\Theta = 0.98$ for $1\,^\circ C < T_\alpha \leqslant 2.2\,^\circ C$,
$\Theta = 0.97$ for $2.2\,^\circ C < T_\alpha \leqslant 5\,^\circ C$ and
$\Theta = 0.95$ for $T_\alpha > 5\,^\circ C$.

The total melt water M_s, expressed in depth units, is given by:

$$M_s = \frac{Q_0}{L_m p_w \Theta},$$

Considering that $L_m = 334.72$ J/g and $p_w = 1$ g/cm^3 then

$$M_s = \frac{Q_0}{334.72\Theta}, \quad (18)$$

In order to compute the melt water M_s, the six components of the Eq. (15) must be estimated as follows:

(i) The Net Radiation Exchange R_N (W/cm^2) is determined by field measurement data of the incoming solar radiation R minus the reflected proportion of radiation which is related to albedo (Baker et al., 1990). Laramie and Schaake (1972) presented a mathematical expression for the albedo curves:

$A = 0.85(0.94)^{(\tau)^{0.58}}$, for the accumulation season,

$A = 0.85(0.82)^{(\tau)^{0.46}}$, for the melt season,

where A is the albedo value and τ is the age of snow surface (the number of days since the last snow storm).

Based on the above, $R_N = R - (1 - A)$.

(ii) The adverted heat Q_V carried by the incoming precipitation depends on its temperature and is expressed as

$$Q_V = C_P p_w P_w T_w \quad (19)$$

where C_P = the specific heat of precipitation [167.36 J/(g °C) if it is snow or 4.184 J/(g °C) if it is rainfall], T_w = the temperature of precipitation (°C), (consider to be equal to the air temperature at 3 m above ground), P_w = the precipitation (cm) and p_w = the density of water (1 g/cm^3).

(iii) The heat consumed in evaporation Q_e is computed as

$$Q_e = p_w L_e E, \quad (20)$$

where L_e is the latent heat of evaporation ($L_e = 597.3 - 0.57\,T_\alpha$) and E is the depth of condensation or evaporation per unit time (cm/day). Evaporation E (cm/day) is given (Bras, 1989) by:

$$E = K_1 (Z_a \times Z_b)^{-\frac{1}{6}} (e_s - e_a) \times u_b,$$

where $K_1 = 0.00651$ [cm/m$^{1/3}$ h/(day h Pa km)], Z_a is the elevation of the snow surface (m), Z_b is the elevation of the overlying air (m), e_s is the saturation vapor pressure at the snow surface (h Pa), e_a is the vapor pressure at elevation a (h Pa) and u_b is the wind velocity at elevation b (km/h). The saturation vapor pressure e_s and the air vapor pressure e_a at the snow surface (a) are computed from:

$$e_s = 0.61078 \times e^{(17.27 \times T)(T + 237.3)},$$
$$e_a = RH \times e_s,$$

where RH is the relative humidity (%) at elevation a, T = air temperature at snow surface (°C).

(iv) The sensible-heat transfer Q_h is proportional to the temperature gradient. The US Army Corps of Engineers recommends:

$$Q_h = C_B P_s \frac{T_a - T_s}{e_a - e_s} \times Q_e, \quad (21)$$

where $C_B = 0.61 \times 10^{-3}$ per °C, P_s is the atmospheric pressure at the snow surface (h Pa), T_a = air temperature at elevation Z_a (°C), T_s = temperature at the snow surface (°C) which is computed using an empirical equation (Li et al., 1999): $T_s = -1.4185\,^\circ C + 0.9844 \times T_a$.

The atmospheric pressure P_s at the snow surface is computed as (Portland State Aerospace Society, 2004):

$$P_s = p_0 \times \exp\left[-\frac{g}{L \times R} \ln\left(\frac{L * a}{T_0} + 1\right)\right],$$

where p_0 is the atmospheric pressure at sea level (mb), g is the acceleration due to gravity (9.806 m/s^2), L is the lapse rate (°C/m), R is the gas constant for air equal to 287.053 J/(kg K), a is the altitude (m), and T_0 is the temperature at zero altitude (°C). The atmospheric pressure p_0 at sea level is equal to 101325 Pa (1 Pa = 0.01 mbar).

(v) Parameter Q_g is the ground-snow exchange by conduction and is related to the heat flux from the soil to the snow pack:

$$Q_g = -K \frac{dT}{dZ}, \quad (22)$$

where K [J/(°C cm day)] is the thermal conductivity of the soil and $\frac{dT}{dZ}$ (°C/cm) is the temperature gradient from soil to snow. The $\frac{dT}{dZ}$ parameter can be calculated experimentally or base on bibliographic references. Q_g ranges between 1.27×10^{-5} and 1.27×10^{-4} cm/day (Eagleson, 1970).

(vi) The freezing of any existing liquid water releases latent heat. The released amount Q_f is computed from:

$$Q_f = \frac{p_p \times D \times W \times L_m}{\Delta t}, \quad (23)$$

where p_p = the snow-pack density (g/cm^3), D = the snow-pack depth (cm), W = the liquid–water content defined as V (water)/V (snow), L_m = the latent heat of freezing (334.72 J/g) and Δt = the time period. According to Bras (1989) the liquid–water content, can be expressed as: $W = (1 - \Theta) \times 100$, where Θ is a thermal quality.

Following the computation of the change in heat storage Q_0 from its components which have been determined above, the snow melt rate M_s was computed from Eq. (18). Finally, the karstic flow discharges from the Stylos Spring were computed from Eqs. (3) and (4) presented in Section "The Karstic model".

The equations of the Energy Budget Snow Melt model take into account the amount of rainfall and the air temperature, but do not take into consideration the topographic characteristics of the mountainous area which affect the snow melt rate, the spatial extents of snow cover and the spatial snow-pack depth. These characteristics must be taken into consideration for the accurate evaluation of the snow melt rate M_s. A GIS snow melt rate model developed for this purpose is presented in the next section.

A snow melt rate model using GIS

The Geographic Information System Arc View 9.2 was used to take topography into consideration. Based on Fig. 5, the karstic area that contributes to the discharge of the Stylos Spring was divided into two parts: (1) one with altitudes <900 m and (2) one with altitudes ⩾900 m (mountainous area). The above division was applied since the relationship between the snowfall percentage (for a given precipitation) and altitude is very low below 900 m elevation

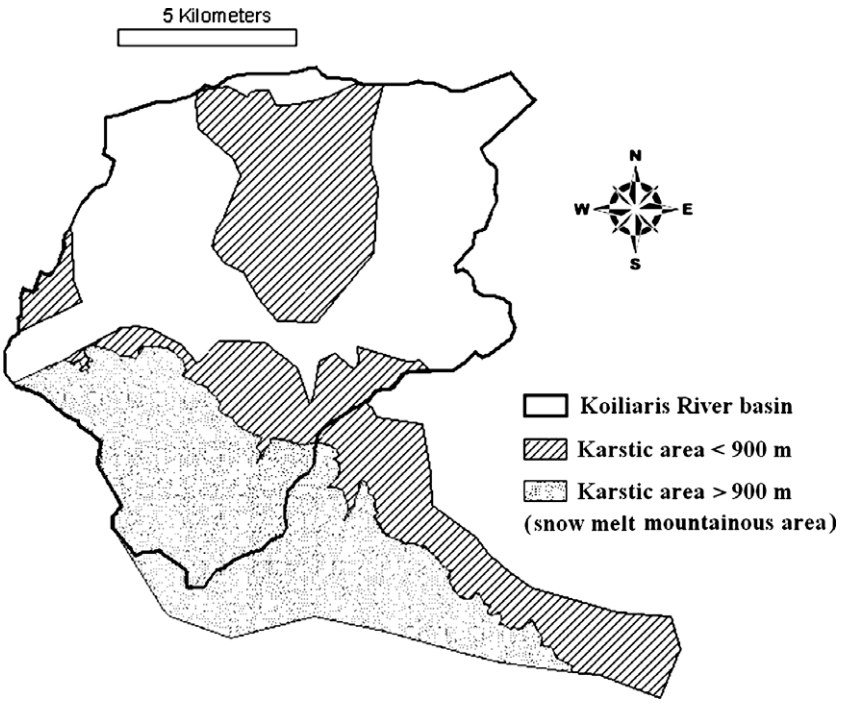

Fig. 5. The karstic area of Koiliaris River Basin divided into two zones above and below 900 ASL.

(Dingman, 1994). The Energy Budget Snow Melt model and the GIS snow melt zone approach were applied only to the karstic area with altitudes $\geqslant$900 m. GIS was used to divide this mountainous area into five different zones characterized by different snow melt rates (very low, low, medium, high, and very high). The final map of the snow melt rate was created based on the topographic characteristics of the area. The snow melt volume Q (m^3/day) for each zone was estimated using the snow melt rate multiplied by the zone area (Nikolaidis et al., 1991):

$$Q = M_s \times A_T, \tag{24}$$

where M_s is the average snow melt rate (m/day) and A_T is the zone area (m^2).

In order to estimate the distribution of the snow melt rate in the karstic area with altitudes above 900 m, seven thematic layer-factors (variables) were created using an Arc Map environment (ESRI, 2006). These thematic layer-factors were: (1) elevation, (2) slope, (3) curvature, (4) aspect, (5) illumination, (6) land use, and (7) solar radiation. All these topographic factors and each separately play a significant role to the snow melt rate. For example in a bare area without land cover the snow melt rate will be very high, contrary to a density land cover in which the snow melt rate will be much smaller (Winkler, 2001). In order to create a uniform indicator of the degree of the snow melt rate, the computed values for each factor were classified on a common scale of vulnerability ranging from 1 to 5.

The five categories for each factor are presented in Table 1. The different levels of these factors are expressed in numerical values for curvature, slope, elevation, illumination and solar radiation, and in descriptive form for aspect and land use. The ranges of the numerical values were based on the Natural Breaks (Jenks) classification method (Smith, 1986).

The description of the effect of a factor depends mainly on its influence on the recharging process. For example, high altitude indicates a very low snow melt rate potential while limited land cover indicates a very high snow melt rate potential. Based on this concept, five major descriptive levels were considered, ranging from Very Low (1 point) to Very High (10 points) (Table 1) and is an expert's judgment that is based on the existing bibliography.

The overall snow melt rate can not be estimated by considering the effect of each factor separately. The integration of all factors is necessary in order to obtain the final snow melt rate map. Since all factors do not have the same degree of influence on snow melt, a weighting approach was adopted where a different weight was assigned to each factor. The methodology presented by Shaban et al. (2001) was employed for the estimation of the factor weights. This method takes into consideration the effect of one factor on all other factors.

A schematic representation of the methodology for each of the seven factors considered in this study is presented in Fig. 6 where two types of effects are considered for each factor: a) the main effect (major avenue), where a change in one factor has a direct effect on another factor, and b) the secondary effect (minor avenue), where a change in one factor has an indirect (secondary) effect on another factor. In order to quantify the two different types of effects, one point was assigned to the main effect and a half point to the secondary (Shaban et al., 2006). Consequently, the summation of points for each factor is as follows:

Elevation	3 major + 2 minor = $3 \times 1 + 2 \times 0.5 = 4.0$ pts
Slope	1 major + 4 minor = $1 \times 1 + 4 \times 0.5 = 3.0$ pts
Aspect	3 major + 0 minor = $3 \times 1 + 0 \times 0.5 = 3.0$ pts
Curvature	3 major + 0 minor = $3 \times 1 + 0 \times 0.5 = 3.0$ pts
Solar radiation	2 major + 1 minor = $2 \times 1 + 1 \times 0.5 = 2.5$ pts
Land use	1 major + 0 minor = $1 \times 1 + 0 \times 0.5 = 1.0$ pts
Illumination	2 major + 1 minor = $2 \times 1 + 1 \times 0.5 = 2.5$ pts

In order to attain a comprehensive evaluation of each factor related to snow melt rate, the rates and weights must be combined. This can be done by multiplying the proposed weight by the rate of effect which yields the total weight of each factor (Shaban et al., 2006). The summation of the total weights yields the grand total

Table 1
Categorization and Calibration of factors affecting snow melt rate in Koiliaris River Basin.

Factor	Descriptive level (snow melt rate)	Proposed weight of effect	Domain of effect
Elevation (m)	Very high	10	<1273
	High	8	1273–1596
	Moderate	5	1596–1867
	Low	3	1867–2072
	Very low	1	2072–2440
Slope (°)	Very high	8	40.47–89.75
	High	6.5	29.56–40.47
	Moderate	5	20.76–29.56
	Low	3.5	8.44–20.76
	Very low	2	0–8.44
Curvature (zunits)	Very high	8	2.29–10.264
	High	6.5	0.58–2.29
	Moderate	5	(−0.65)–0.58
	Low	3.5	(−2.43)–(−0.65)
	Very low	2	(−9.47)–(−2.43)
Aspect	Very high	8	South
	High	6.5	Southwest
	Moderate	5	West
	Low	3.5	East, southeast, northwest
	Very low	2	North, northeast
Illumination (0–255)	Very high	8	208–254
	High	6.5	172–208
	Moderate	5	136–172
	Low	3.5	98–136
	Very low	2	0–98
Land use	Very high	8	Bare rock
	High	6	Sparsely vegetated areas
	Moderate	5	Natural grassland
	Low	4	Vegetation with low and closed cover
	Very low	3	Sclerophyllous vegetation (subforest)
Solar radiation (WH/m^2)	Very high	8	1.217.269–1.429.258
	High	6.5	1.072.224–1.217.269
	Moderate	5	927.179–1.072.224
	Low	3.5	776.555–927.179
	Very low	2	6.700–776.555

weight (Table 2). The last column of Table 2 shows the percentage contribution of each factor to the snow melt rate, that is, the ratio of the total weight to the grand total.

The resulting map of snow melt includes the combination of the above seven variables that are related directly to the snow melt rate. Specifically, the produced seven maps were combined using a weighted linear combination approach in a GIS environment.

Based on this technique each map (factor) is multiplied by its weight (percentage) and then summed to yield the final snow melt map S (Gemitzi et al., 2006):

$$S = \sum w_i x_i, \tag{25}$$

where w_i is the weight of factor i (percentage) and x_i is the factor map i.

The final objective was to create a snow melt rate map for the extended karstic area of the Koiliaris River Basin that contributes to the discharge of the Stylos Spring. The final snow melt map S, disaggregates spatially the results of the snow melt rate in Eq. (18). Next, based on Eq. (25) and Tables 1 and 2, these maps were combined with the weighting approach of thematic levels (GIS) aiming at the creation of the final snow melt rate map. According to the above methodology the area was divided into six karstic zones (five zones with snow melt and the one without snow melt). The main characteristics of these six zones were logged to the Energy Budget Snow Melt model. The estimated values of precipitation and of the snow melt flow of the six karstic areas were finally used as input to the Maillet karstic model.

A MATLAB code that incorporates the previous models

A MATLAB code was developed to incorporate the equations of the two-part karstic model. Specifically, the code combines Eqs. (5)–(31) which are related to the Energy Budget Snow Melt model. Recall that the karstic area was divided into six zones based on the GIS snow melt rate model. For each of these zones, the daily rainfall and temperature were computed and imported as a text file to the MATLAB code model. The output values of each run were aggregated in order to determine the final discharge from the Stylos Spring, which was subsequently used as input to the HSPF Model. A friendly GUI (Graphical User Interface) was also developed to provide an interface between the user and the application's underlying code. The HSPF model has the ability to simulate the surface flow from the basin to the river. The final objective of this study was the simulation of the total flow (surface and groundwater) of the Koiliaris River Basin.

The HSPF model

The Hydrological Simulation Program – FORTRAN (HSPF) simulates the hydrologic and associated water quality processes on pervious and impervious land surfaces, in streams and in well-mixed impoundments. The model simulates the time response of the watershed based on the hydrologic and geochemical mass balance and the wet and dry depositions to the surface water. The HSPF model is a physical model that incorporates GIS data (Bicknell et al., 2001).

The HSPF model operates in the frame of the BASINS model. The new edition (2007) of the BASINS 4 model was used in this work. The BASINS 4 model allows for the division of a basin into sub-basins, and, therefore, can simulate the hydrology of the entire basin in a more accurate manner. The essential geographic information required by the BASINS 4 model is the watershed, the sub-basins, the hydro network, the land uses and the ground surface elevations. This information was supplied to the model through GIS. The basin of the Koiliaris River was divided into six sub-basins (SWS1–SWS6) as shown in Fig. 7. The main criteria for selecting these six sub-basins were the uniform hydrologic, topographical, geological and land-planning characteristics. The above sub-basin information becomes the input for the BASINS-4 model which creates the data files in the form required by the HSPF model. In addition, the Watershed Data Management (WDM) program was used to log all the meteorological time series required for the HSPF model.

Different time series regarding temperature and rainfall were used for each sub-basin. These time series were related to the annual rainfall gradient and the monthly temperature gradient for the region of interest. The necessary meteorological data used were: temperature, dew point temperature, solar radiation, wind speed, precipitation, potential evapotranspiration and evaporation. All these data had an hourly time step as required by the HSPF model for the accurate simulation of rain events (Bicknell et al., 1993). The input requirements for all sub-basins were provided to the HSPF model by using the BASINS 4 model. The time series of the karstic discharge from the Stylos Spring were input to the code in order to calculate both the surface and underground discharges.

A disadvantage of the HSPF model is the fact that it can not simulate the flow along karstic channels where significant water losses occur. The part of the Koiliaris River Basin along the Diktamos Gorge (Fig. 1) has a karstic geological formation. Therefore, the simulation of the flow along this channel is particularly difficult

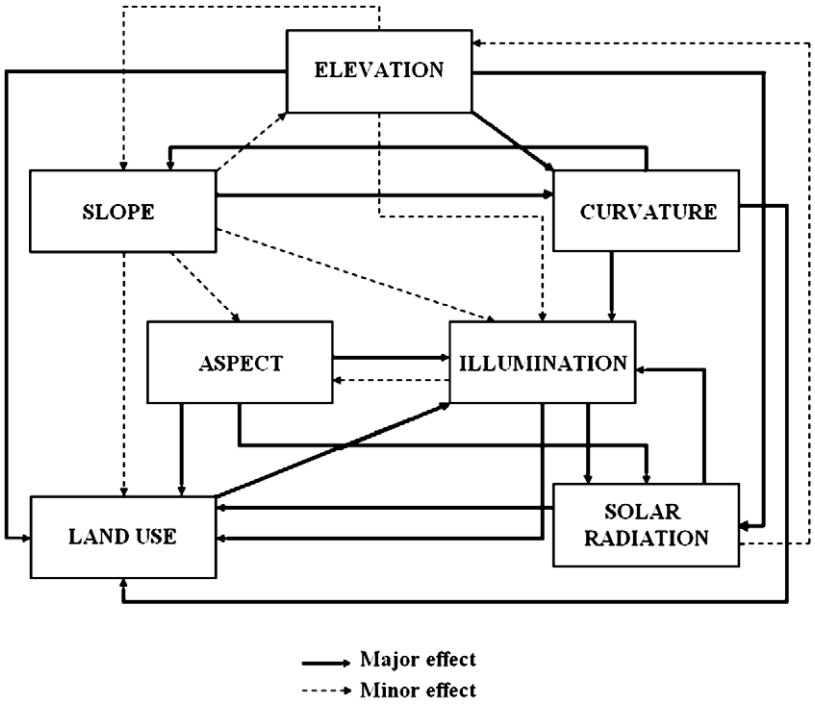

Fig. 6. Schematic depiction of interaction of factors that influence the territorial snow melt rate.

Table 2
Weight evaluation of factors influencing snow melt rate.

Factor	Descriptive scale (snow melt rate)	Weight (a) (1–10)	Rate (b)	Weighted rating ($a * b$)	Total weight	Present %
Elevation (m)	Very high	10	4	40	108	22.314
	High	8		32		
	Moderate	5		20		
	Low	3		12		
	Very low	1		4		
Slope (%)	Very high	8	3	24	75	15.496
	High	6.5		19.5		
	Moderate	5		15		
	Low	3.5		10.5		
	Very low	2		6		
Curvature (zunits)	Very high	8	3	24	75	15.496
	High	6.5		19.5		
	Moderate	5		15		
	Low	3.5		10.5		
	Very low	2		6		
Aspect	Very high	8	3	24	75	15.496
	High	6.5		19.5		
	Moderate	5		15		
	Low	3.5		10.5		
	Very low	2		6		
Illumination (0–255)	Very high	8	2.5	20	62.5	12.913
	High	6.5		16.25		
	Moderate	5		12.5		
	Low	3.5		8.75		
	Very low	2		5		
Land use	Very high	8	1	8	26	5.372
	High	6		6		
	Moderate	5		5		
	Low	4		4		
	Very low	3		3		
Solar radiation (WH/m^2)	Very high	8	2.5	20	62.5	12.913
	High	6.5		16.25		
	Moderate	5		12.5		
	Low	3.5		8.75		
	Very low	2		5		
					Sum = 484	Sum = 100

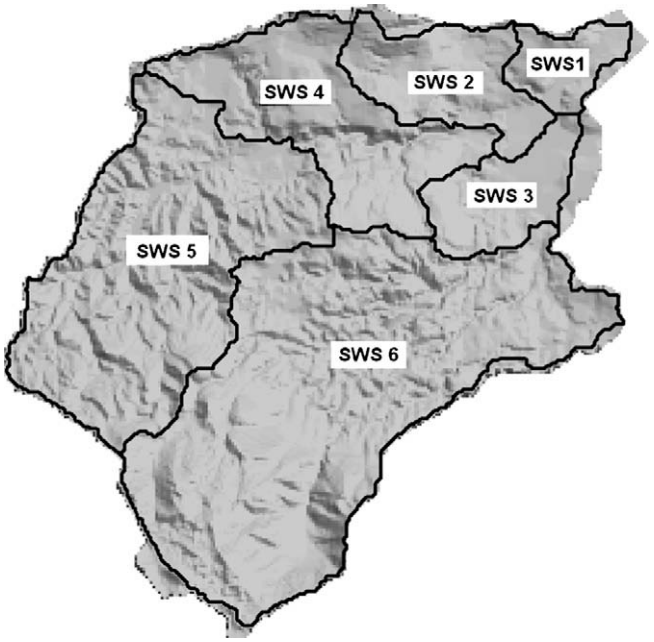

Fig. 7. The six (6) sub-basins of the Koiliaris River Basin.

by using the HSPF model alone. For this reason, an empirical hydrologic loss model was developed.

The empirical hydrologic loss model for a karstic river channel

The flow data at the entrance (inflow) and the exit (outflow) of the Diktamos Gorge (sub-basin SWS 4) were collected from two telemetric hydrometric stations–Faraggi and Stylos, respectively–for the time period 01/07/2007–31/8/2008.

The hydrologic balance equations presented in Section "The Karstic model" were modified and applied as follows:

$$\frac{dV}{dt} = Q_{in} - Q_{out} + (P \times A_r) - (L_{oss} \times A_r), \tag{26}$$

$$\frac{dV}{dt} = Q_{in} - Q_{out} + (P \times A_r) - (I + E) \times A_r, \tag{27}$$

where $\frac{dV}{dt}$ is the water volume change rate (m^3/day), Q_{in} and Q_{outt} are the inflow and outflow (m^3/day) from SWS 4, respectively, P is the precipitation (m), A_r is the river area (m^2), and L_{oss} = the water losses along the karstic channel which are expressed as the summation of infiltration (I) and evaporation (E). Since the change rate of the water volume along the river channel is equal to zero (assuming steady state during each time step = 1 h), Eq. (27) yields:

$$Q_{out} = Q_m + (P \times A_r) - (I + E) \times A_r. \tag{28}$$

The area of the watercourse of this karstic river channel has been estimated to be 105,000 m^2 (4200 m × 25 m).

The evaporation was determined by using the Penman empirical equation:

$$E = 1.63 \times 10^{-9} \times (0.93 + U_{wind}) \times (e_s - e_0), \tag{29}$$

where E is the evaporation (cm/day), U_{wind} is the wind speed (m/day), e_s is the atmospheric saturated pressure (h Pa), and e_0 is the atmospheric pressure (h Pa).

The infiltration rate along the karstic channel was computed by using the Kostiakov empirical equation:

$$I = B \times t^{-n}, \tag{30}$$

where I is the infiltration (cm), B = Kostiakov's time coefficient term (cm/day) and n = Kostiakov's time exponent term (dimensionless), t = time simulation (day). Based on Eq. (30), when $t \to 0$, $I \to \infty$ and when $t \to \infty$, $I \to 0$.

Parameters B and n in Eq. (30) were determined by using linear regression approaches. The combination of Eqs. (28)–(30) yields the final equation that describes the hydrologic balance losses in the karstic part:

$$Q_{out} = Q_{in} + (P \times A_r) - ((3.9 \times 10^{-3} \times t^{1.2105} + 1.63 \times 10^{-9} \times (0.93 + U_{wind}) \times (e_s - e_0)) \times A_r \tag{31}$$

Results and discussion

The GIS energy budget snow melt-karstic model

The extended karstic area that contributes to the Stylos Spring was estimated to be 107 km^2. Fig. 8 shows the snow melt rate maps for each of the snow melt factors and the final 3-D snow melt rate map. It should be noticed that the snow melt factors refer only to the areas where snowfall occurs (altitude above 900 m). Table 3 presents the areas and the mean altitudes for the six zones of the karstic region. The above information was used in the energy budget snow melt-karstic model for each of the six sub-basins of the Koiliaris River Basin and the graphical representation of the obtained results is shown in Fig. 9.

The HSPF-empirical karstic channel model

Calibration and validation

The hydrologic simulation was performed for the time period 09/01/2006–31/08/2008. For this time period, hourly data for the flow were available from the hydrometric station of sub-basin SWS 1. For the time period 01/07/2007–31/08/2008, hourly data for the flow were also available from the hydrometric stations of Faraggi and Stylos, at the entrance and exit of sub-basin SWS 4, respectively. The required inputs were supplied to the HSPF model and the model was simulated. Parameter calibration was performed following the simulation. The simulation results were introduced to the BASINS model for analysis by using the Scenario Generator (GenScn) software tool.

Calibration is an iterative process used in establishing the most suitable values for some model parameters (Albek et al., 2004). In this study, the calibration was performed manually for the time period 01/09/2007–31/8/2008 and the obtained parameters were used for model validation for the time period 09/01/2006–31/8/2007.

The following HSPF model parameters were used for the calibration (Kim et al., 2007): (a) the lower zone nominal soil moisture storage (LZSN) which is related to both precipitation patterns and soil characteristics, (b) the nominal upper zone soil moisture storage (UZSN) which is related to land surface topography, (c) the mean soil infiltration rate (INFLT), (d) the lower zone of evapotranspiration (LZETP), and (e) the groundwater recession flow parameters (KVARY) which are used to describe non-linear groundwater recession flow. The first step in the calibration process was the calculation of the hydrologic parameters for sub-basin SWS 5, at the exit. The flow results obtained by using the HSPF are compared to the field data in Fig. 10.

The results obtained by using the empirical hydrologic loss model (Eq. (31)) for the hydrologic years 2007–2008 are in good agreement with the observed field data (Fig. 11).

The flow data at the exit (outflow) of the Diktamos Gorge (SWS 4) was computed by applying the empirical karstic channel model (hydrologic loss model) for the entire simulation time period (09/

01/2006–31/8/2008) (Fig. 12). In this case, the input flow data Q_{in} in Eq. (31) was the calibrated outlet flow value of the HSPF model for sub-basin SWS 5.

During the calibration time period, the annual flow at the entrance point of the Diktamos Gorge (SWS 4) was estimated to be 12.11 million m^3/year. The annual flow at the outlet point was 1.47 million m^3/year (12.14%) and the losses along the karstic channel of the Diktamos Gorge were 10.64 million m^3/year (87.86%).

Final results and the reliability of the conceptual model

The model described in Section "The empirical hydrologic loss model for a karstic river channel" was developed in order to calculate the flow time series Q_{out} at the outflow point of the Diktamos Gorge (karstic channel). The subtraction of this flow data from the calibrated outlet flow of the HSPF model at sub-basin SWS 5 yields the flow time series related to water losses (Q') along the karstic channel. This loss data must be subtracted from the final computed flow of the HSPF model at the outflow point of SWS 4. The comparison of the HSPF model results to the field data for sub-basin SWS 1 is presented in Fig. 13. Based on these results (unified framework model), the average annual flow in sub-basin SWS 1 was estimated to be 5.85 m^3/s which is in very good agreement with the observed value of 6.07 m^3/s (error of 3.62%).

The annual hydrologic mass balance for the karstic system and the Koiliaris River watershed during the calibration time period was estimated as follows. The annual flow at the exit point of the basin outlet was 136.29 million m^3/year. The karstic flow contribution was 109.059 million m^3/year (80%) and the watershed flow was 31.5 million m^3/year. After evapotranspiration losses (4.20 million m^3/year), the net contribution of watershed flow to the river was 27.3 million m^3/year (20%). The total rainfall that entered the extended karstic system was estimated to be 269 million m^3/year and the snow melt was 30.2 million m^3/year.

In order to compare the field data with the simulation results in Fig. 13, the Root Mean Squared Error (RMSE) was used, defined as:

$$\mathrm{RMSE} = \sqrt{\frac{1}{n} * \sum_{i=1}^{n} R_i^2},$$

where R_i is the difference between the observed data and the fitted model for the ith sample. Values of RMSE close to zero indicate perfect fit and the model calibration is considered satisfactory only when RMSE < 3.0.

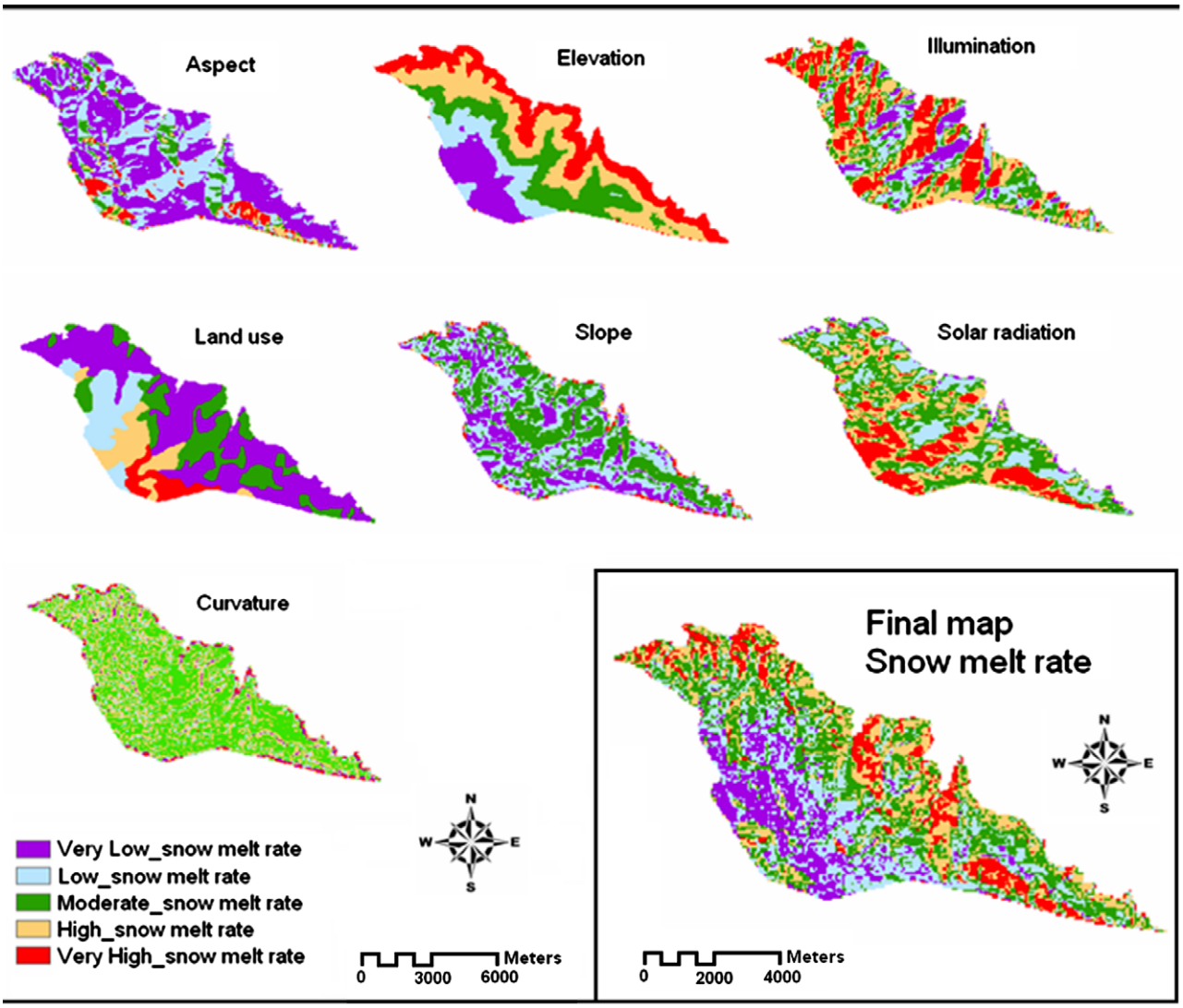

Fig. 8. A graphical representation of the territorial snow melt rate for each snow melt factor and the final snow melt rate map.

Table 3
The characteristics of the six karstic zones.

Karst area ⩾900 m altitude	Zones	Mean elevation (m)	Area (m^2)
Very high snow melt	1	1480	9391250.365
High snow melt	2	1574	23015342.03
Medium snow melt	3	1630	29013194.17
Low snow melt	4	1737	31304156.63
Very low snow melt	5	1894	15554472.25
Karst area <900 m altitude	6	620	59405635.43

Another indicator used for the comparison of field data and simulation results is the Normalized Root Mean Squared Error (RMSE):

$$\text{Normalized RMSE} = \frac{\text{RMSE}}{(X_{\text{obs}})_{\max} - (X_{\text{obs}})_{\min}}.$$

The Normalized RMSE indicator is expressed as a percentage and is more representative than the RMSE indicator since it takes into consideration the range of field data values. For example, an RMSE value equal to 1.5 indicates non-accurate calibration of the model for observed values between 10 and 20, but implies excellent calibration for observed values between 100 and 200. On the other hand, the Normalized RMSE is equal to 15% in the first case and equal to 1.5% in the second case.

Besides these two indicators, we also use the determination index R^2 for the comparison of field data and simulation results. R^2 takes values between 0 and 1; the higher the value of R^2, the better the relation between simulation results and field data. A model calibration is considered satisfactory when $R^2 \geqslant 0.80$ (Coulibaly and Baldwin, 2005).

In the case of our model, the following values were obtained for the calibration time period: $R^2 = 0.92$, RMSE = 1.19 and Normalized RMSE = 0.00167%. Also, the Kolmogorov–Smirnov statistic test (K–S test) was used, that compares the (cumulative) distributions of the model and filed data (Eadie et al., 1971). The Maximum difference in cumulative probability (K–S test) for the calibration time period was equal to 0.14 m^3/s, and the correlation coefficient = 0.96. In addition, the Nash–Sutcliffe coefficient of efficiency

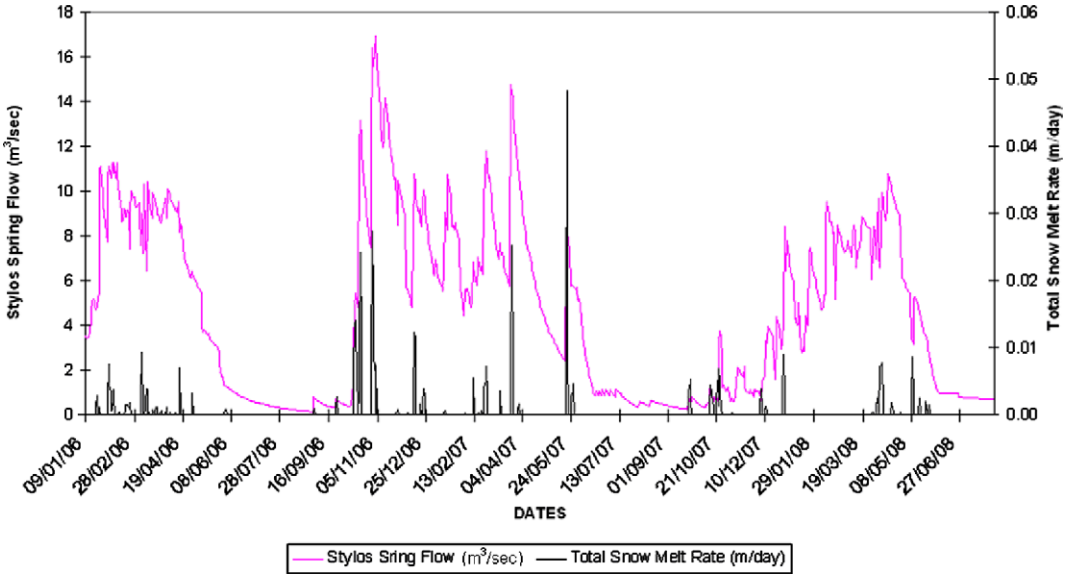

Fig. 9. The calculation of the daily spring flow and total snow melt rate.

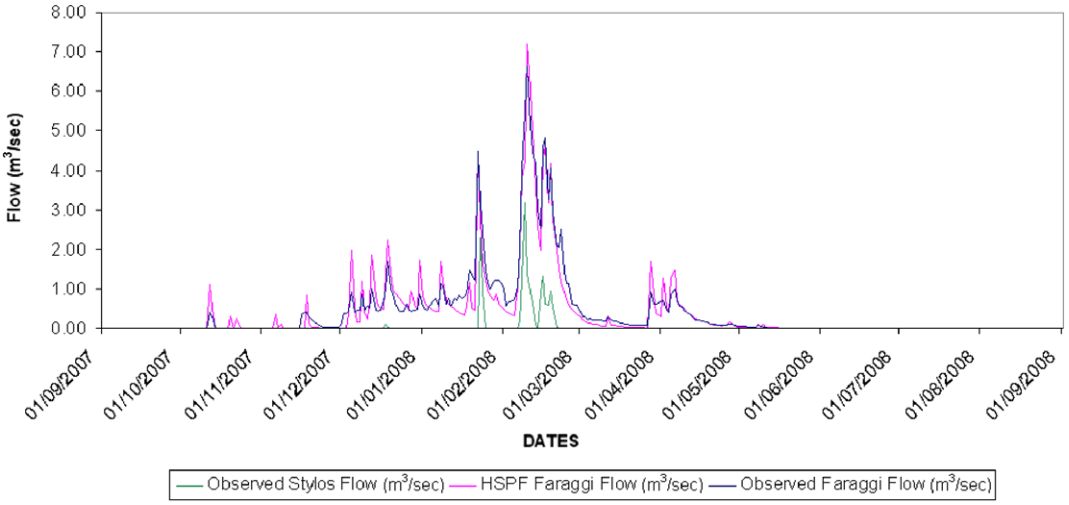

Fig. 10. Daily flow observations (SWS 5–SWS 4) and model results (SWS 5).

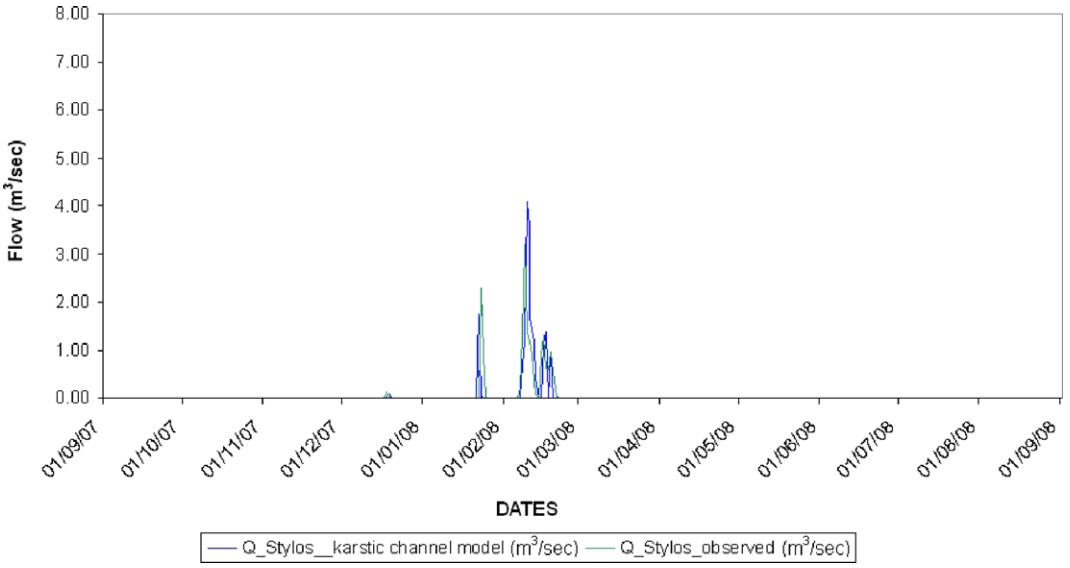

Fig. 11. Daily flow observations and model results (SWS 4).

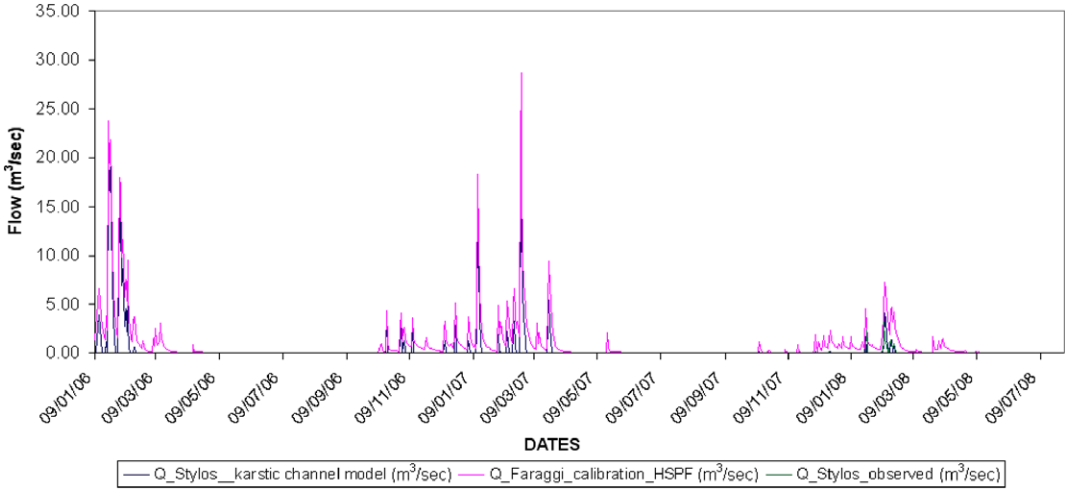

Fig. 12. Daily flow model results (SWS 4–SWS 5).

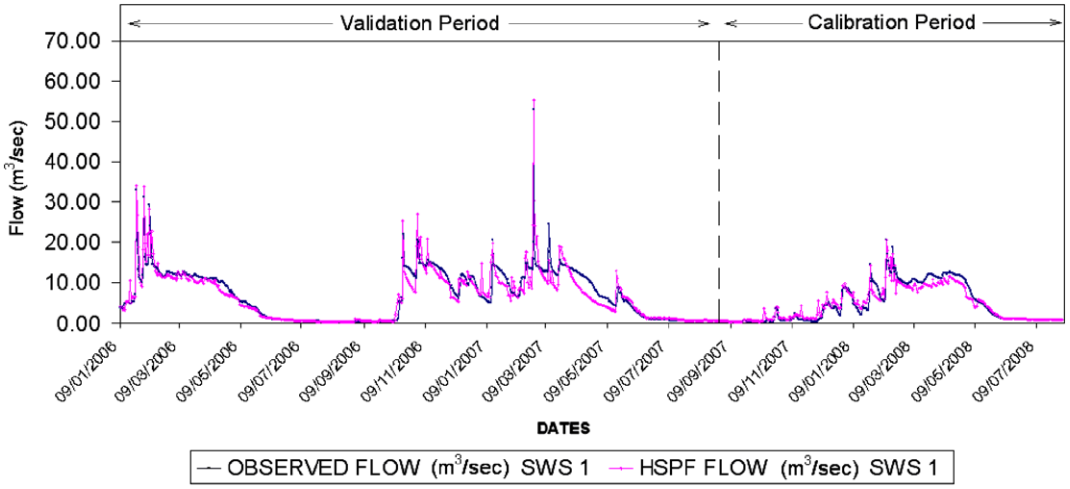

Fig. 13. Daily flow observations and model results (SWS 1).

(NS index) was computed, which is a measure of the quality of the model with respect to the representation of the variance of the data (Nash and Sutcliffe, 1970). A value of 1 of the NS index means that the representation is perfect. In the present simulation the NS index for the calibration time period was equal to 0.91. All the above statistical parameters show a very good agreement between simulated results and field measurements.

For the validation time period the R^2 index was equal to 0.86, the RMSE = 2.49, the Normalized Root Mean Squared indicator = 0.00134%, the K–S test = 0.129 m^3/s, the Correlation coefficient = 0.94 and the NS index = 0.87.

A sensitivity analysis of the HSPF model was also performed to study the sensitivity of the calibrated results in comparison to the field data (Al-Abed and Whiteley, 2002). The main calibrated hydrologic parameters were disturbed by ±10%, in order to calculate the sensitivity of each parameter. The sensitivity index S used in this part of the study was defined as:

$$|S| = \frac{\frac{Q_{new} - Q_{calibrated}}{Q_{calibrated}}}{\frac{K_{new} - K_{calibrated}}{K_{calibrated}}},$$

where K_{new}, $K_{calibrated}$ are the new and calibrated values for hydrologic parameter K of the HSPF model and Q_{new}, $Q_{calibrated}$ are the simulation values for K_{new} and $K_{calibrated}$, respectively. The lower the value of S, the lower the sensitivity of parameter K is. Based on the analysis results, the mean soil infiltration rate INFILT (S = 0.00327) appears to be the most sensitive parameter, followed by the nominal upper zone soil moisture storage UZSN (S = 0.00092), the lower zone nominal soil moisture LZSN (S = 0.12), the lower zone of evapotranspiration LZETP S = 0.00044), and the groundwater recession flow parameters KVARY (S = 0.00019).

The simulated flows suggest that the proposed framework for hydrological analysis of complex hydromorphological systems is capturing the processes operating in the basin. The underlying principle in developing the framework was based on field data collected at points within the watershed where the intersection of geologic and morphologic systems occur. Each sub-model of the framework was calibrated with a unique hydrologic data-set in order to capture the hydrologic variability of the response of the subsystem. The calibration and validation data-sets used represent different conditions in order to ensure that we get the right answers for the right reasons (Kirchner, 2006). In addition, the overall goodness of fit was evaluated. This procedure was used in order to minimize the uncertainty inherent in the simulation results and establish evidence for the uniqueness of the proposed parameterization. For example, the karstic model parameterization was based on geologic evidence of two types of karst existing in the area (Plakenkalt and Tripali limestones) as well as hydrologic analysis of the behaviour of the springs using four years of continues hydrologic data. This work improved the previous hydrologic analysis by developing a spatially distributed snow model. The consistency of the response of the karstic system in time makes us confident of the reliability of the simulated results as well as of the uniqueness of the model parameters. Similarly, the reliability of the HSPF model simulation was examined by conducting a sensitivity analysis on the model parameters. The low sensitivity (10% change in a parameter produced less than 0.3% change in the simulated flow) of the model parameters suggests that the calibrated parameters represent at least local minima. The low sensitivity in combination with the experience obtained during the calibration procedure suggests that the simulated hydrologic pathways are appropriate and the selected model parameters are unique. Finally, the modeling of the transmission losses in the karstic gorge was based on a combination of mass balance equation and flow parameterization, calibrated with two years of continuous flow data. Complex hydromorphologic environments require use of combination of system specific models in order to reduce the uncertainty and the uniqueness of the simulated results.

Conclusions

The aim of this study was the development of a framework to model the hydrologic processes in a complex hydrogeological river basin such as the Koiliaris River Basin (Prefecture of Chania, Crete). Due to the complex karstic geomorphology of the system which has a significant contribution to the Koiliaris River flow in the form of groundwater flow, a combination of models was used. In karstic river basins the contribution of the subsurface flow can be a significant portion of the total flow and has a complex behaviour that is difficult to model. More specifically, in order to improve the agreement between simulation results and field data, the HSPF model was combined with a MATLAB code model that incorporates a two-part Maillet karstic model, a GIS-based energy budget snow melt rate model and an empirical karstic channel flow model. As expected, the snow melt rate plays an important role regarding the final form of the hydrograph and the agreement of the simulated hydrograph peaks to the observed field data. The results obtained in the present study showed a very good agreement with field measurements.

In complex geomorphological karstic river basins, the climatic changes may cause extreme phenomena (floods and droughts). One of the main parameters that affect the generation of these phenomena is the snow melt rate. The framework model presented in this study, in contrast to other integrated hydrologic models, takes into consideration all the components that affect the snow melt process. Specifically, among the other parameters that affect the snow melt energy budget, the topography is taken into consideration using GIS and by incorporating seven important parameters that play an important role in the snow melt process. These seven parameters were the elevation, slope, curvature, aspect, illumination, land use, and radiation. The main contributions of the present work includes the combination of the HSPF model with a karstic model, the development of an empirical karstic channel flow model and a GIS-based energy budget snow melt rate model. The karstic models, developed in the present work, can easily be adapted to any karstic terrain. Also, the GIS-based energy budget snow melt rate model can be used for any mountain river basin where snow melt occurs. The above models can become useful to the mountain hydrology developments for a better description of the complex processes that take place in the physical system. Also, since flood phenomena have occurred from time to time in the area of study, the present model could become a useful tool for the prediction of flood events and for the better management of water supplies.

References

Al-Abed, N.A., Whiteley, H.R., 2002. Calibration of the hydrological simulation program Fortran (HSPF) model using automatic calibration and geographical information systems. Hydrological Processes 16, 3169–3188.

Albek, M., Öğütveren, U., Albek, E., 2004. Hydrological modeling of Seydi Suyu watershed (Turkey) with HSPF. Journal of Hydrology 285, 260–271.

Anderson, E.A., 1968. Development and testing of snowpack energy balance equations. Water Resources Research 4, 19–37.

Anderson, E.A., 1973. National Weather Service River Forecast System – snow accumulation and ablation model, NOAA Technical Memorandum NWS-HYDRO-17, United States Department of Commerce, National Oceanic and Atmospheric Administration, National Weather Service, Washington, DC, USA.

Baker, D.G., Ruschy, D.L., Wall, D.B., 1990. The albedo decay of prairie snows. American Meteorological Society 29, 179–187.

Bicknell, B.R., Imhoff, J.C., Kittle Jr., J.L., Donigian Jr., A.S., Johanson, R.C., 1993. Hydrological Simulation Program – FORTRAN. User's Manual for Release 10. EPA Environmental Research Laboratory, Athens, GA.

Bicknell, B.R., Imhoff, J.S., Kittle, J.L., Jobes, T.H., Donigian, A.S., 2001. Hydrological Simulation Program – FORTRAN (HSPF): User's Manual –Version 12. National

Exposure Research Laboratory, Office of Research and Development, US Environmental Protection Agency, Athens, Georgia, USA.
Bras, L.R., 1989. Hydrology: An Introduction to Hydrologic Science. Massachusetts Institute of Technology.
Coulibaly, P., Baldwin, C.K., 2005. Nonstationary hydrological time series forecasting using nonlinear dynamic methods. Journal of Hydrology 307, 164–174.
Dingman, S.L., 1994. Physical Hydrology. Prentice-Hall, New Jersey.
Eadie, W.T., Drijard, D., James, F.E., Roos, M., Sadoulet, B., 1971. Statistical Methods in Experimental Physics. North-Holland, Amsterdam. pp. 269–271.
Eagleson, P.S., 1970. Dynamic Hydrology. McGraw-Hill, New York.
ESRI, 2006. ArcView 9.2 User Manuals, Environmental System Research Institute, 380 New York Street, Redlands, CA 92373, USA.
Ganju, A., Satyawali, P.K., Singh, A., Sethi, D.N., 1999. Snowcover simulation model – a review. Defence Science Journal 49 (5), 419–436.
Gemitzi, A., Petalas, C., Tzihrintzis, V.A., Pisinaras, V., 2006. Assessment of groundwater Vulnerability to pollution: a combination of GIS, fuzzy logic and decision making techniques. Environmental Geology 49, 653–673.
Jaquet, O., Siegel, P., Klubertanz, G., Benabderrhamane, H., 2004. Stochastic discrete model of karstic networks. Advances in Water Resources 27, 751–760.
Kim, S.M., Benham, B.L., Brannan, K.M., Zeckoski, R.W., Doherty, J., 2007. Comparison of hydrologic calibration of HSPF using automatic and manual methods. Water Resources Research 43, W01402.
Kirchner, W.J., 2006. Getting the right answers for the right reasons: linking measurements, analysis, and models to advance the science of hydrology. Water Resources Research 42, W03S04. doi:10.1029/2005WR004362.
Kourgialas, N.N., Karatzas, P.G., Nikolaidis, P.N., 2008. Simulation of the flow in the Koiliaris River basin (Greece) using a combination of GIS, the HSPF model and a karstic – snow melt model. In: 4th Biennial International Congress of iEMSs, Barcelona Spain, vol. 1, pp. 512–520.
Laramie, R.L., Schaake, J.C., 1972. Simulation of the Continuous Snowmelt Process. MIT Department of Civil Engineering, Cambridge, MA (Technical report no. 143).
Li, Shusun, Zhou, X., Morris, K., 1999. Measurement of snow and sea ice surface temperature and emissivity in the Ross Sea. IEEE Journal (0-7803-5207-6/99).
Maillet, E., 1905. Essais d' hydraulique sonterraine et fluviaie. Herman, Paris.
Mazurkiewicz, A.B., Callery, D.G., McDonnell, J.J., 2008. Assessing the controls of the snow energy balance and water available for runoff in a rain-on-snow environment. Journal of Hydrology 354, 1–14.
Nash, J.E., Sutcliffe, J.V., 1970. River flow forecasting through conceptual model. 1: discussion of principles. Journal of Hydrology 10 (3), 282–290.
Nikolaidis, P.N., Nikolaidis, V.S., Schnoor, J.L., 1991. Assessment of episodic freshwater acidification in the Sierra Nevada, California. Aquatic Sciences 53 (4), 330–345.
Ohara, N., Kawas, M.L., 2005. Field observations and numerical model experiments for the snowmelt process at a field site. Advances in Water Resources 29, 154–160.
Portland State Aerospace Society, 2004. A Quick Derivation relating altitude to air pressure. Version 1.03.
Sensoy, A., Sorman, A.A., Tekeli, A.E., Sorman, A.U., Garen, D.C., 2006. Point-scale energy and mass balance snowpack simulations in the upper Karasu basin, Turkey. Hydrological Processes 20, 899–922.
Shaban, A., Khawlie, M., Bou Kheir, R., Abdallah, C., 2001. Assessment of road instability along a typical mountainous road using GIS and aerial photos, Lebanon-eastern Mediterranean. Bulletin of Engineering Geology and the Environment 60, 93–101.
Shaban, A., Khawlie, M., Abdallah, Ch., 2006. Use of remote sensing and GIS to determine recharge potential zones: the case of Occidental Lebanon. Hydrogeology Journal 14, 433–443.
Smith, R.M., 1986. Comparing traditional methods for selecting class intervals on choropleth maps. The Professional Geographer 38 (1), 62–67.
Stamati, F., Nikolaidis, N., Bozinakis, K., Papamastorakis, D., Kritsotakis, M., 2006. Stochastic modeling of the karstic system of western Apokoronas in Crete. In: VIII International Conference Protection and Restoration of the Environment VIII, Chania, Greece, pp. 184–192.
Tzoraki, O., Nikolaidis, N.P., 2007. A generalized framework for modeling the hydrologic and biogeochemical response of a Mediterranean temporary river basin. Journal of Hydrology 346, 112–121.
US Army Corps of Engineers, 1956. Snow Hydrology. Department of Commerce, Office of Technical Services, Washington, DC (PB 151660).
Viswanathan, C., Teegavarapu, R.S., Ormsbee, L., 2005. Surface water assessment and hydrologic modeling under Karst aquifer conditions. In: American Geophysical Union Conference, November–December 2005, AGU Conference, San Francisco, USA.
White, W.B., 2002. Karst hydrology: recent developments and open questions. Engineering Geology 65 (2–3), 85–105.
Winkler, R.D., 2001. The effects of forest structure on snow accumulation and melt in South-Central British Columbia. Degree of Doctor of Philosophy the University of British Columbia.
Yang, Z.-L., Dickinson, R.E., 1997. Validation of the snow submodel of the biosphere–atmosphere transfer scheme with Russian snow cover and meteorological observational data. Journal of Climate 10, 353–373.